

# Supporting information for:

## Nonlinear Rheological Behaviors in Confined Polymer Melts after Step Shear

Yongjin Ruan,<sup>†,‡</sup> Yuyuan Lu,<sup>\*,†</sup> Lijia An,<sup>\*,†,‡</sup> and Zhen-Gang Wang<sup>\*,¶,†</sup>

<sup>†</sup>State Key Laboratory of Polymer Physics and Chemistry, Changchun Institute of Applied Chemistry, Chinese Academy of Sciences, Changchun 130022, People's Republic of China

<sup>‡</sup>University of Chinese Academy of Sciences, Beijing 100049, People's Republic of China

<sup>¶</sup>Division of Chemistry and Chemical Engineering, California Institute of Technology, Pasadena, CA 91125, United States

E-mail: yylu@ciac.ac.cn; ljan@ciac.ac.cn; zgw@caltech.edu

### S1 Effects of shear rate

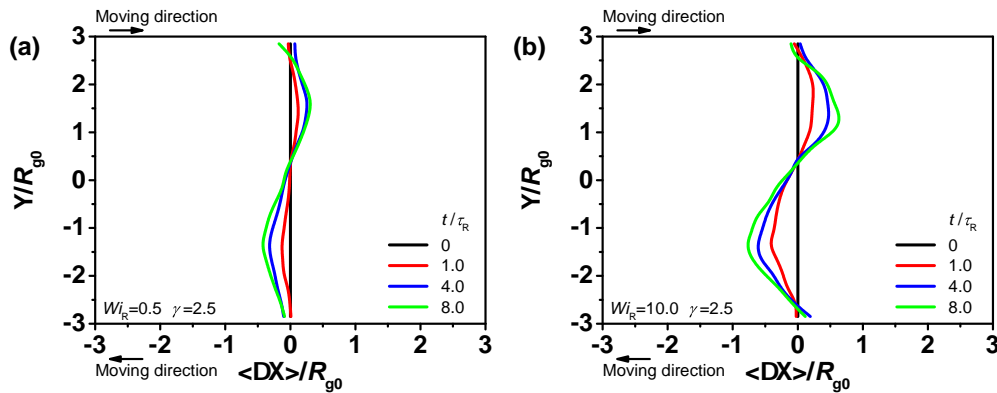


Figure S1: Displacement along the flow direction at step strain  $\gamma = 2.5$  with (a)  $Wi_R = 0.5$  and (b)  $Wi_R = 10.0$ . The higher shear rate results in larger displacement.

## S2 Self-diffusivity $D$ and Rouse self-diffusivity $D_R$

In Figure S2, we plot the product  $6DN$  vs.  $N$ . The plateau value 0.52 for chains with no stiffness at short chain lengths correspond to Rouse dynamics. Rouse self-diffusivity  $D_R$  is then obtained from  $6D_R N = 0.52$ . For chains with stiffness  $K = 2.0$ , the product  $6DN$  also converges to 0.52 for short chain lengths, so the Rouse self-diffusivity  $D_R$  is determined similarly.

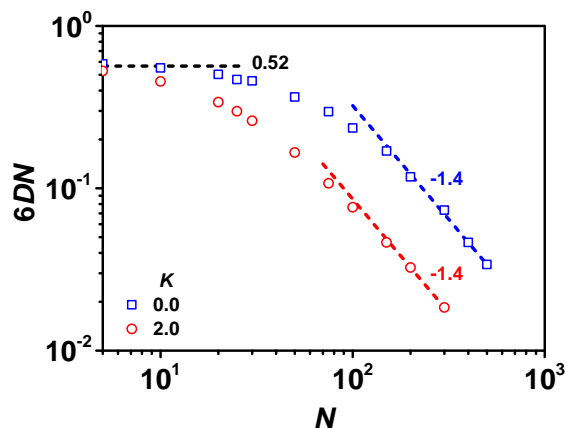


Figure S2: The product  $6DN$  vs.  $N$  for different bending stiffness.

## S3 Relaxation moduli

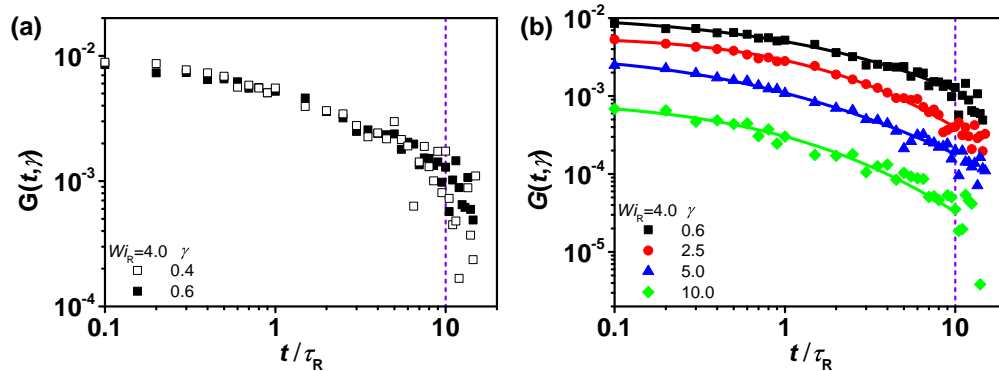


Figure S3: Relaxation moduli with  $Wi_R = 4.0$ . The magnitudes of shear strain  $\gamma$  are: (a) 0.4 and 0.6, (b) 0.6, 2.5, 5.0 and 10.0 from top to bottom, the solid lines are obtained from polynomial fitting based on the least square method using data in the range from  $0.1\tau_R$  to  $10\tau_R$ .

## S4 The fracture of different samples

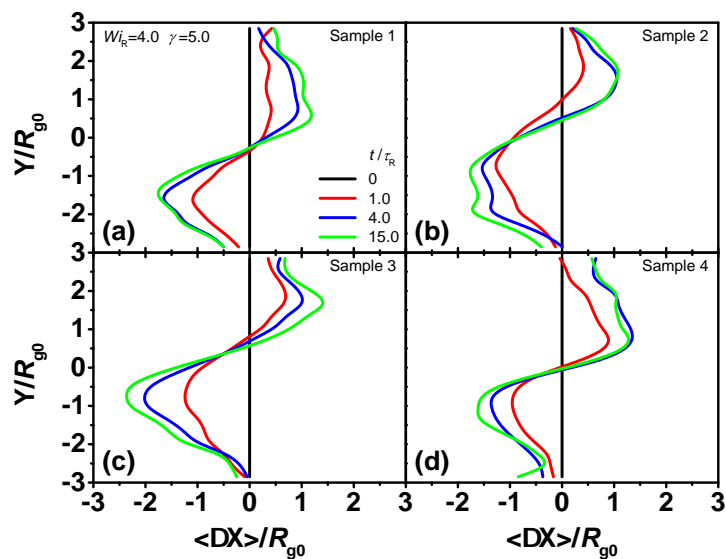


Figure S4: Displacements along the flow direction in four different samples after a step strain of  $\gamma = 5.0$ . The corresponding movie can be found in Movie S2.

## S5 Effects of thermal noise

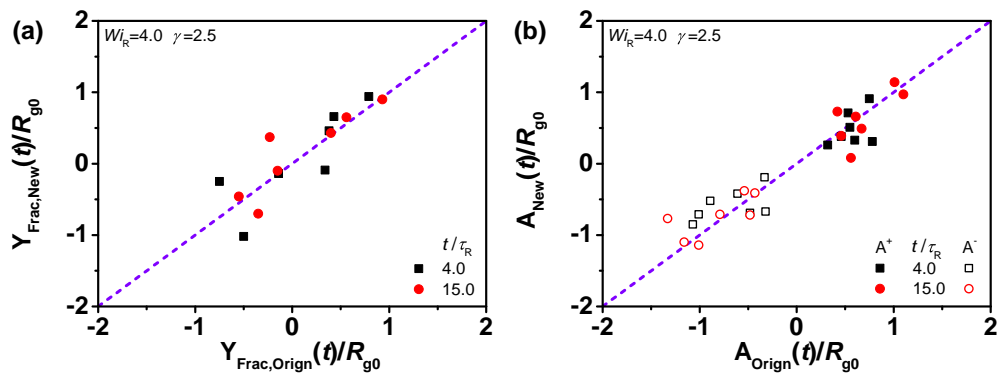


Figure S5: Comparison of (a) the original fracture position ( $Y_{\text{Frac,Orign}}$ ) with the new fracture position ( $Y_{\text{Frac,New}}$ ), and (b) the original maximum displacement of macroscopic motions ( $A_{\text{Orign}}$ ) with the new maximum displacement ( $A_{\text{New}}$ ).  $A^+$  and  $A^-$  are, respectively, the maximum displacements in the positive and negative directions.

## S6 Effects of chain stiffness

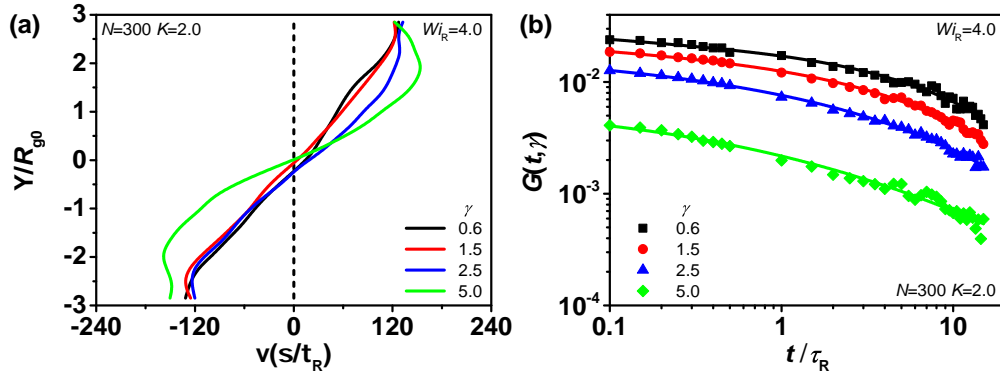


Figure S6: (a) Velocity profiles of the average displacements of the free-chain monomers for  $N = 300$  and  $K = 2.0$  in the gradient direction during a step shear with  $Wi_R = 4.0$ . Note that the profile deviates significantly from being linear, signaling shear banding in the system. (b) Relaxation moduli with  $Wi_R = 4.0$ . The magnitudes of shear strain  $\gamma$  are 0.6, 1.5, 2.5 and 5.0, the solid lines are obtained from polynomial fitting based on the least square method using data in the range from  $0.1\tau_R$  to  $15\tau_R$ .

## S7 Comparison between the boundary conditions

For comparison, we also performed startup shear using the *fix deform* command in LAMMPS. The stress-strain behavior and the velocity profiles are shown in Figure S7. The effect of the walls on the stress is quite weak, while there is more visible difference in the velocity profile, the latter probably reflecting effects of the grafted chains. Non-quiescent relaxation is also observed in the periodic systems upon shear cessation, as shown in Figure S8.

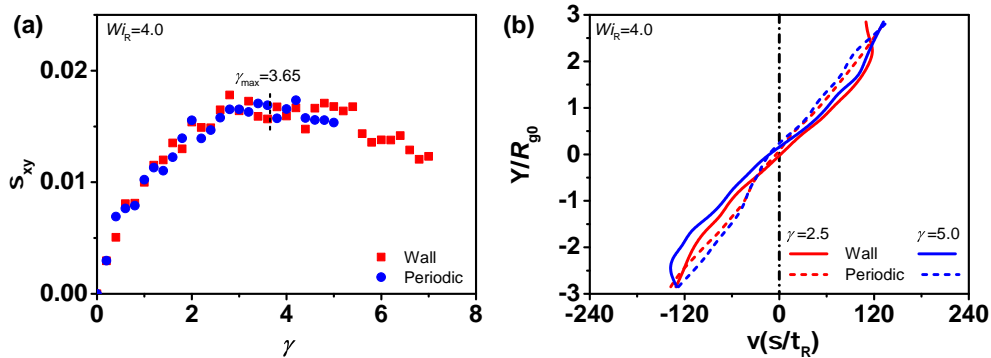


Figure S7: (a) Stress vs. strain and (b) velocity profiles, with wall-driven and *fix deform* deformation protocols.

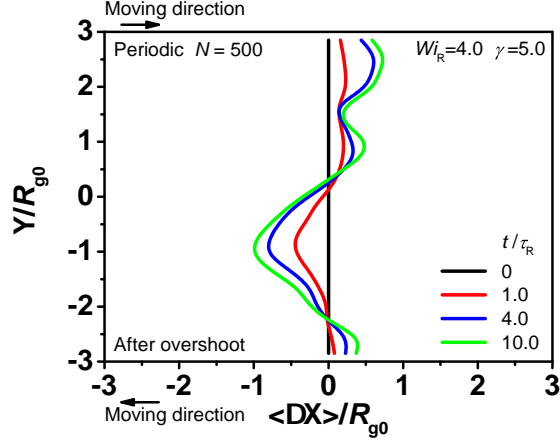


Figure S8: Displacements along the flow direction in one sample after a step strain of  $\gamma = 5.0$  with the *fix deform* deformation protocol.

## S8 The finite size effects

To ensure that the results reported in the main text with box size  $6 \times 6 \times 4$  (where the dimensions are in units of radius of gyration  $R_{g0} = \sqrt{\langle R_{g0}^2 \rangle}$ ) are not due to finite size effects, we also performed simulations using two larger box sizes  $12 \times 6 \times 4$  and  $6 \times 12 \times 4$ . The effect of the box size on the stress and velocity profile is weak (Figure S9). The increase of the flow direction has no influence on the layer displacements as shear stops (Figure S10 (a)), while the change in the gradient direction enhances the layer displacements (Figure S10 (b), the vertical axis is normalized by the box size)

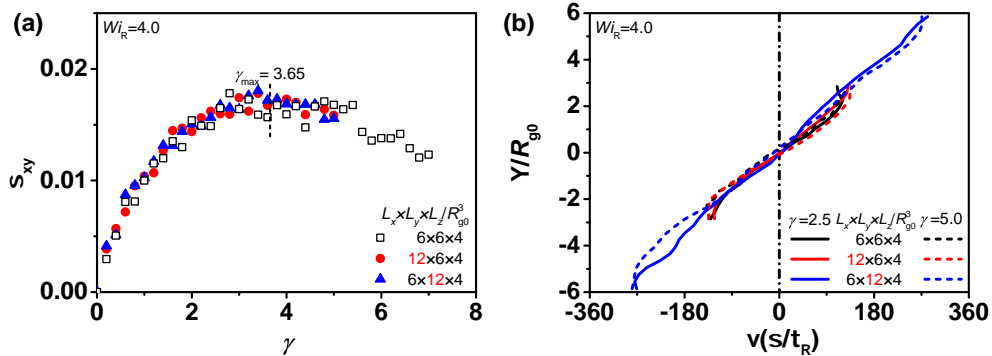


Figure S9: (a) Stress vs. strain and (b) velocity profiles under different box sizes. The dimensions of the box size are in unit of  $R_{g0}$ .

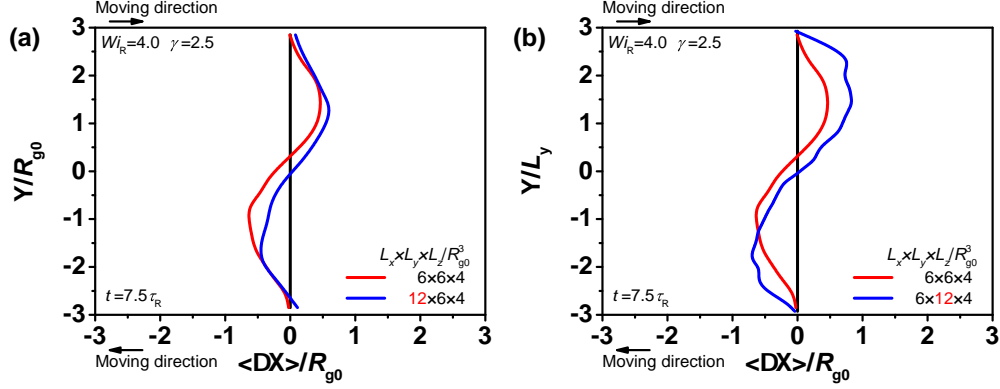


Figure S10: Layer displacements along the flow direction at step shear  $\gamma = 2.5$  under different box sizes. The dimensions of the box size are in unit of  $R_{g0}$ .  $L_y$  is the simulation box size in the gradient direction.

## S9 Description of movies

Movie S1 and Movie S2 respectively show the motion of the center of mass (CM) of each free polymer chain under the conditions of  $Wi_R = 4.0$  and  $\gamma = 2.5$  (Movie S1) or  $\gamma = 5.0$  (Movie S2) in the  $xy$  plane with a window size of  $6R_{g0} \times 1.5R_{g0}$ , where the white balls represent the polymer chains whose CMs are located in the frame at the moment of shear cessation; the red and green balls represent the polymers whose CMs move into the frame from the left and right during flow, respectively.